TITLE:

Schizophrenia Exhibits Bi-Directional Brain-Wide Alterations in Cortico-Striato-Cerebellar Circuits

AUTHOR LIST:

Jie Lisa Ji[1], Caroline Diehl[1], Charles Schleifer[1], Godfrey Pearlson[1], Genevieve Yang[1], Gina Creatura[1], John H. Krystal[1], Grega Repovs[2], John Murray[1], Anderson Winkler[3], Alan Anticevic[1]

1. Department of Psychiatry, Yale University School of Medicine, 300 George Street, New Haven, CT 06511, USA
2. Department of Psychology, University of Ljubljana, Ljubljana, Slovenia
3. Oxford University, John Radcliffe Hospital, Headington, Oxford OX3 9DU, UK

Corresponding Author:

Alan Anticevic, Yale University, Department of Psychiatry
40 Temple St Ste 6E, New Haven, CT 06520
alan.anticevic@yale.edu

Word Count: 7028

ABSTRACT

Distributed neural dysconnectivity is considered a hallmark feature of schizophrenia, yet a tension exists between studies pinpointing focal disruptions versus those implicating brain-wide disturbances. The cerebellum and the striatum communicate reciprocally with the thalamus and cerebral cortex through monosynaptic and polysynaptic connections, forming cortico-striatal-thalamic-cerebellar (CSTC) functional pathways that may be sensitive to brain-wide dysconnectivity in schizophrenia. It remains unknown if the same brain-wide pattern of alterations persists across CSTC systems, or if specific alterations exist along key functional elements of these networks. We characterized whole-brain cerebellar and striatal connectivity using resting-state functional magnetic resonance imaging in 159 chronic schizophrenia patients and 162 matched controls, along each major cerebellar and striatal functional subdivision. Both cerebellar and striatal associative subdivisions revealed consistent brain-wide bi-directional alterations in patients relative to controls, marked by hyper-connectivity with bilateral sensory-motor cortices and hypo-connectivity with association cortex. These results implicate a consistent motif of brain-wide alterations in cortico-striato-cerebellar systems in schizophrenia, calling into question accounts of exclusively focal functional connectivity disturbances.

Key Words: cerebellum; striatum; schizophrenia; connectivity; resting-state; fMRI

INTRODUCTION

A fundamental challenge in clinical neuroscience is the search for robust neuroimaging biomarkers reflecting disease-related alterations in large-scale neural systems. Advances in human neuroscience offer opportunities for clinical translations and biomarker development. For instance, emerging human neuroimaging studies have identified the presence of large-scale cortico-striatal-thalamic-cerebellar (CSTC) functional pathways that are stable and replicable across hundreds of individuals[1-3]. Such pathways may be particularly sensitive to disruptions in psychiatric illness such as schizophrenia (SCZ), which has been conceptualized as a disorder of synaptic communication affecting distributed neural systems. Leading theoretical models of SCZ propose that disruptions in local microcircuit excitation (E) and inhibition (I) neuronal balance, stemming from altered glutamatergic signaling, may underlie observed alterations across neural systems[4-6]. One possibility is that such alterations occur only in select CSTC functional pathways if such pathways are more vulnerable to the upstream microcircuit perturbations. Alternatively, such synaptic perturbations may generalize across distributed CSTC pathways. A major gap in knowledge concerns whether neural disturbances in SCZ manifest brain-wide across CSTC functional pathways, or if they occur in only select CSTC regions. Resolving this tension is critical to informing biomarker development that can guide rational treatment for either targeted neuropathology in specific areas or diffuse alterations that span CSTC pathways.

One widely replicated effect in SCZ neuroimaging is the disruption in functional relationships involving the thalamic resting-state blood-oxygen-level-dependent (BOLD) signal. The thalamus consists of topographically organized nuclei that are densely connected with other brain areas[7-9], making it highly sensitive to widespread disturbances in functional circuits. Specifically, several independent replications have established elevated alterations in correlated BOLD signal fluctuations between the thalamus and sensory neural networks[10-12]. In contrast, the same studies identified reductions in thalamic coupling with associative cortical areas. These effects generalize across patients with chronic SCZ and those at ultra-high-risk for developing SCZ[13]. Critically, these effects are most pronounced along higher-order associative thalamic functional subdivisions (e.g. mediodorsal nucleus). Multiple theoretical models have proposed that these disruptions in thalamic functional coupling may be a hallmark of the illness[14]. Yet, it remains unknown if these disrupted patterns manifest across the entire CSTC functional pathway or if they are exclusive to the thalamus. Put differently, is the disruption in BOLD signal covariation seen in SCZ specific to the thalamus, or does it generalize to other CSTC functional systems due to their shared relationships with thalamic and cortical networks? If the thalamic effect is indeed specific and unique, then similar patterns would not be expected to emerge across other systems as robustly. However, if SCZ involves synaptic neural alterations that are not exclusive to the thalamus (but affect shared pathways) then we hypothesize that the aforementioned effects observed with the thalamus will emerge across all brain-wide CSTC systems as a shared and robust pattern of disruption. Previous studies have identified alterations in isolated regions of the basal ganglia and cerebellum in SCZ[15-24], but to date none have examined whether disturbances in functional relationships are unified across these neural systems.

A way to close this knowledge gap involves leveraging existing resting-state findings in healthy humans that have defined large-scale functional networks across cortical, striatal and cerebellar neural territories[1-3]. This work implicated a shared functional architecture across the CSTC systems that can be used to assay patterns of changes across each functional CSTC subdivision in SCZ. Using the striatal or cerebellar elements of each functional network allows comprehensively characterizing altered functional relationships across CSTC systems while bypassing the thalamus as a starting point. Notably, the cerebellum does not share monosynaptic anatomical connections with cortex, thalamus or striatum (i.e. in a strict sense is not a part of the anatomically-defined cortico-striatal-thalamic-cortical loop). However, it is highly functionally connected these areas via polysynaptic pathways, as evidenced by stable and cohesive large-scale functional networks across these neural territories[1-3]. Hence the cerebellum is uniquely placed to serve as a control in our study: if an effect is detected with the cerebellum, it would support the hypothesis that disruptions in SCZ are indeed pervasive across functional brain-wide networks, and not limited by thalamic or striatal anatomy *per se*.

We identified bi-directional CSTC dysconnectivity patterns previously shown in SCZ when using the thalamus as a starting point. This effect was robust and highly conserved across both the cerebellar and

striatal functional subdivisions. This robust, conserved, and pervasive CSTC dysconnectivity in SCZ rules out the possibility of exclusive thalamic disruptions. Results further revealed that the disturbance is most pronounced along higher-order associative divisions of the CSTC networks, using both an independently defined *a priori* parcellation and a fully data-driven clustering approach. Collectively, these results strongly implicate a diffuse neuropathology in SCZ impacting all elements of the CSTC pathway but a preferentially more severe disruption of higher-order associative networks – in line with leading theoretical models of the illness.

RESULTS

Bi-directional Brain-wide Cerebellar and Striatal Dysconnectivity is Observed in SCZ. To test whether SCZ is associated with uniform disturbances across CSTC networks, we quantified whole-brain functional connectivity of spontaneous BOLD signals with 7 cerebellar and 6 striatal functionally distinct parcels[2, 3]. Each parcel is a component of one of 7 large-scale functional networks that were first discovered and then validated in samples of 500 healthy adults respectively[1-3]. Critically, these networks show corresponding elements across cortical, cerebellar, and striatal territories. **Fig. 1a** highlights the *a priori* functional networks in the cerebral cortex (middle), cerebellum (left panel) and striatum (right panel), from the parcellations derived by Yeo et al. (2011)[1], Buckner et al. (2011)[2] and Choi et al. (2012)[3]. This parcellation contains both <u>*sensory*</u> networks (visual, VIS and somatomotor, SOM) and <u>*associative*</u> networks (dorsal attention, DAN; ventral attention, VAN; limbic, LIM; frontoparietal control, FPCN; and default mode, DMN) (**Supplementary Fig. S1**). Below, we use the term "parcel" to refer to a region of the cerebellum or striatum defined by its membership in one of the 7 functional networks. Of note, no representation of the visual network was discovered in the striatum[3]; hence only 6 striatal parcels were used across all striatal analyses.

Here we studied a well-powered sample of patients diagnosed with chronic SCZ (N=159) and matched healthy controls (CON, N=162; see **Supplementary Table S1** for detailed demographics). First, we computed a 2x7 *Group* x *Parcel* ANOVA to test for differences in functional connectivity across the 7 cerebellar network parcels between SCZ and CON groups (see **Online Methods** and **Supplementary Fig. S2** for unthresholded Z-maps of all seeds). All reported whole-brain effects survived non-parametric threshold-free-cluster-enhancement (TFCE) correction[25] with 2,000 permutations (see **Online Methods**). Henceforth we use the term 'dysconnectivity' to denote the difference between SCZ and CON groups in the statistical covariation of BOLD signals over time across regions. Between-group differences revealed cerebellar hyper-connectivity with somatomotor cortex in SCZ relative to CON, and hypo-connectivity with prefrontal cortex, thalamus and striatum (**Fig. 1b-c**; see **Supplementary Fig. S4a-b** for unthresholded maps). **Fig. 1d** highlights the shift in the distribution of cerebellar connectivity strengths in SCZ for both hyper-connected and hypo-connected regions and the group difference in mean connectivity of these regions. An independent 2x6 *Group* x *Parcel* ANOVA was computed for the 6 functional striatal parcels (see **Supplementary Fig. S3** for unthresholded Z maps of all network parcels). Between-group differences revealed qualitatively similar dysconnectivity patterns as with cerebellar parcels, namely hyper-connectivity with somatomotor cortex and hypo-connectivity with frontal cortex, thalamus, and cerebellum (**Fig. 1e-f;** see **Supplementary Fig. S4c-d** for unthresholded map). **Fig. 1g** highlights the shift in the distribution of striatal connectivity strengths in SCZ for both hyper-connected and hypo-connected regions and the group difference in mean connectivity of these regions. Repeating analyses without global signal regression did not alter key effects (**Supplementary Fig. S5**). As expected, differences across parcels (i.e. main effect of *Parcel* irrespective of group) revealed widespread differential coupling for both cerebellar and striatal analyses, indicating that connectivity patterns across parcels differ (**Supplementary Fig. S6**). Critically, the reported CSTC between-group effects were not explained by smoking status, head motion, signal-to-noise ratio, or medication dose (**Supplementary Fig. S7**). Between-group effects adjusted for motion and signal-to-noise, as well as the effects of these covariates, are reported in **Supplementary Fig. S8-S9**.

Notably, there were no significant correlations between the degree of dysconnectivity across patients (hyper-connectivity, hypo-connectivity, or a linear combination of the two) and SCZ symptom severity (as measured by the Positive and Negative Symptom Scale (PANSS)). This absence held for individual symptoms

(**Supplementary Fig. S10-S11**) as well as when using the classic three-factor model of the Positive and Negative Syndrome Scale – a well-established measure of symptoms across the psychosis spectrum (PANSS, positive, negative, and general symptoms[26]; see **Supplementary Fig. S12-S13**, $p>0.05$ with Bonferroni correction). To ensure a comprehensive characterization of symptom-related effects, we additionally investigated the relationship between identified dysconnectivity and an alternative five-factor model of PANSS, shown to be stable in an external sample of 5,789 subjects[27]. These additional analyses again revealed weak correlations between the degree of dysconnectivity and the five-factor model symptom solution (**Supplementary Fig. S14a-b** & **S15a-b**). These comprehensive symptom analyses suggest that the identified CSTC dysconnectivity likely constitutes a trait-like effect, as opposed to a robust state-like marker, in line with prior observations that revealed modest relationships with thalamic connectivity[12]. Put differently, these brain-wide differences do not reflect patients' current symptom status, but may rather indicate a stable, disease-associated change.

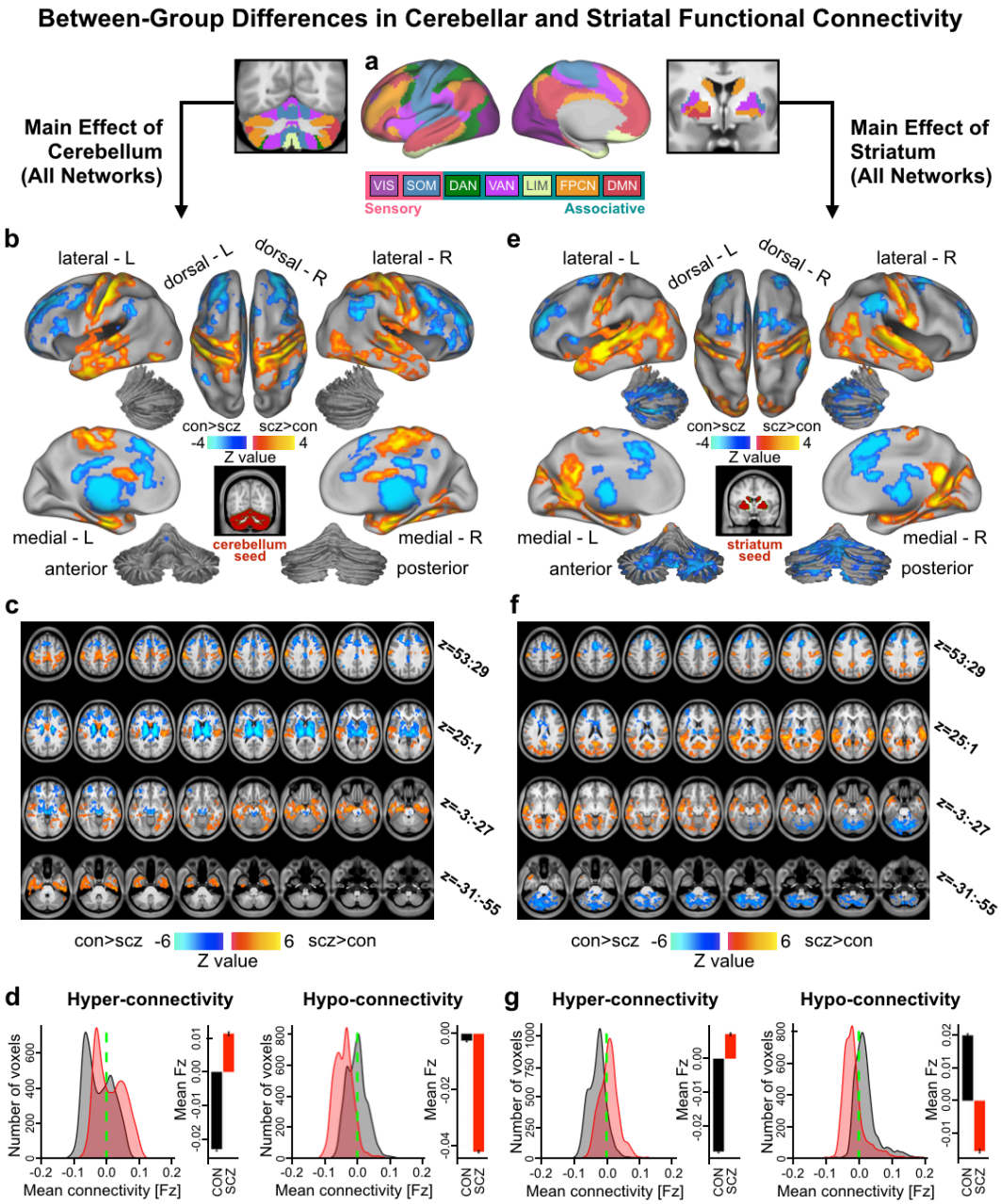

Figure 1. Main effect of cerebellar and striatal network parcel connectivity in SCZ. (a) Functionally defined networks obtained from 1,000 resting-state scans (first defined and independently replicated in 500 scans respectively) in the cerebral cortex, cerebellum and striatum[1-3]. Whole-brain functional connectivity was computed from each of these 7 network parcels in the cerebellum (6 in striatum) and quantified in a *Group* (SCZ vs. CON group) x *Parcel* (VIS, SOM, DAN, VAN, LIM, FPCN and DMN) ANOVA. Networks were broadly grouped as either sensory or associative. **(b)** Cortical surface view of areas showing significant main effect of *Group* in whole-brain connectivity with the cerebellar parcels *(p*<0.05 TFCE whole-brain corrected) between 159 patients with chronic schizophrenia (SCZ) and 162 healthy controls (CON). Orange/yellow areas indicate regions where patients exhibited stronger cerebellar connectivity, whereas blue areas indicate regions where patients exhibited reduced cerebellar connectivity, relative to controls. Inset shows coverage of all cerebellar parcels. **(c)** Volume-based axial view of cerebellar connectivity group differences in **b** with Z-coordinate ranges (each slice in each row increments by 3 mm). **(d)** Distribution of connectivity strength (Fz) values within voxels showing significant hyper- and hypo-connectivity in SCZ and CON. Bar plots show mean connectivity averaged across all voxels in hyper- and hypo-connected areas. **(e-g)** Results for identical independent analysis conducted with the 6 functionally-defined striatal network parcels. Note that there was no representation of the visual network in striatum[3] and therefore that network was omitted. Abbreviations: VIS, visual network; SOM, somatosensory; DAN, dorsal attention network; VAN, ventral attention network; LIM, limbic network; FPCN, frontoparietal control network; DMN, default mode network.

Next, given the marked qualitative similarity between the cerebellar and striatal dysconnectivity maps (**Fig. 2a**, **Supplementary Fig. S4**), we formally quantified the overlap between the two independent *a priori* analyses. This was achieved by computing the correlation between the two group difference maps (expressed as difference in Fz values), but after removing cerebellar and striatal voxels from their respective maps. A significant positive relationship (r=0.40, p<0.001) indicated high similarly between striatal and cerebellar dysconnectivity in SCZ (**Fig. 2b**). We also quantified the cerebellar and striatal dysconnectivity overlap for areas showing significant hyper-connectivity (yellow) and hypo-connectivity (blue) (**Fig. 2c & d**). **Fig. 2e** indicates high overlap across both cerebellar and striatal hyper-connectivity effects (orange areas indicate overlapping effects, logical OR; yellow areas indicate joint effects, logical AND). Notably, the number of voxels in the overlapping areas was above chance (hypergeometric test for probability of overlap, p<0.001, given the total number of voxels in the brain) (**Fig. 2f**, see **Online Methods**). Similarly, **Fig. 2g** indicates the same result for hypo-connectivity effects (dark blue areas indicate overlapping effects, logical OR; light blue areas indicate joint effects, logical AND). Again, the number of hypo-connected voxels that overlapped between cerebellar and striatal analyses was above chance (p<0.001, **Fig. 2h**). Overall, quantitatively and spatially high similarity between cerebellar and striatal dysconnectivity suggests highly comparable brain-wide perturbations.

Figure 2. Similarity between perturbed cerebellar and striatal connectivity in SCZ. (a) Surface unthresholded Z-maps showing cerebellar and striatal between-group connectivity differences. Qualitatively, regions that exhibited an increase in cerebellar connectivity in SCZ also exhibited an increase in striatal connectivity, and vice versa. **(b)** Scatterplot showing a highly significant positive relationship between group differences in cerebellar and striatal whole-brain connectivity (r=0.40, p<1.00e-15). The plot shows Fz values for all voxels in cerebellar (X-axis) and striatal (Y-axis) between-group connectivity maps. **(c)** Surface maps of conjunction analysis showing areas that are significantly hyper-connected (yellow) and hypo-connected (blue) with both cerebellar and striatal parcels. **(d)** Volume-based axial view of **a** with Z-coordinate ranges (each slice in each row increments by 3 mm) **(e)** Surface view of areas showing both significant cerebellar (cbm) and striatal (str) hyper-connectivity (logical AND, bright yellow) and areas significantly hyper-connected to one or the other (logical OR, orange). **(f)** The number of voxels overlapping between observed cerebellar and striatal hyper-connectivity maps is significantly greater than chance *(p*<0.001), given the total number of voxels in the brain. **(g)** Surface view of areas showing both significant cerebellar (cbm) and striatal (str) hypo-connectivity (logical AND, bright blue) and areas significantly hypo-connected to one or the other (logical OR, dark blue). **(h)** Number of voxels that overlap between observed cerebellar and striatal hypo-connectivity maps is significantly greater than chance *(p*<0.001), given the total number of voxels in the brain. Dashed red lines in **f** and **h** indicate 95% Clopper-Pearson confidence intervals for chance.

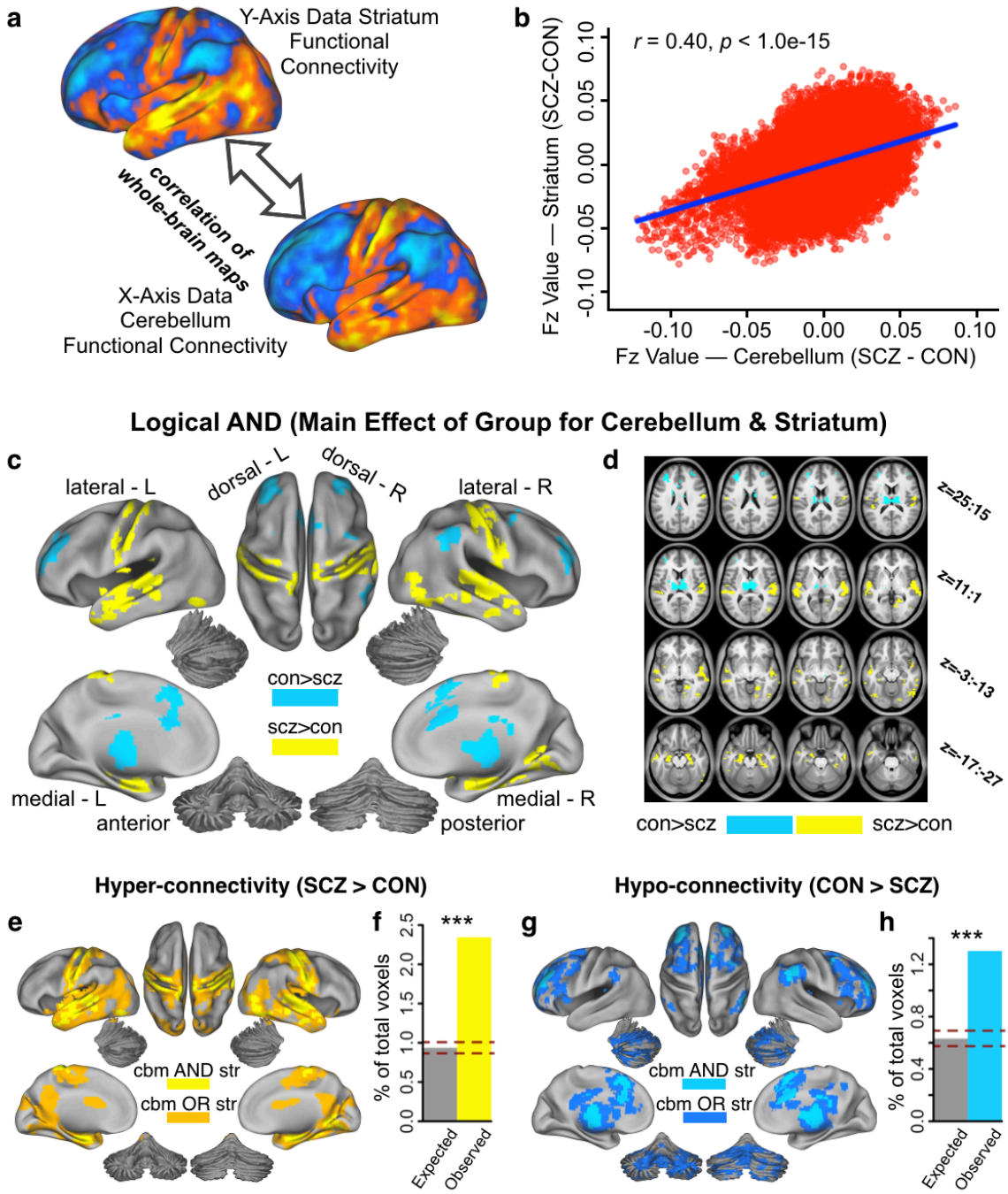

Dysconnectivity in SCZ is Driven by Associative Network Disruptions. Prior analyses are highly consistent with the hypothesis that CSTC disruptions in SCZ are robust and highly conserved across both the cerebellar and striatal systems. However, it remains unknown if these alterations are preferential to some functional networks that span both cerebellum and striatum. For instance, prior work strongly implicates associative network disturbances in SCZ in the cerebral cortex[4, 28, 29]. Yet, to our knowledge, no study has tested if such disruptions persist in a uniform pattern across the associative networks for both cerebellum and striatum. To test this we computed a *Group x Parcel* interaction, which would explicitly reveal differential between-group disruptions across distinct cerebellum and striatum parcels. The cerebellar *Group* x *Parcel* interaction effect revealed 37 areas throughout the brain (**Fig. 3a**). In turn, the striatal *Group* x *Parcel* interaction effect revealed 60 areas throughout the brain (**Fig. 3e**). These effects suggest that between-group dysconnectivity was not uniform across all parcels for either the cerebellar or striatal analyses. Importantly,

these whole-brain interaction effects did not solely depend on within-cerebellum or within-striatum interactions (see **Online Methods** and **Supplementary Fig. S17-S19**). Next, we tested for the source of the interaction and examined if the interaction effect was consistent for both cerebellum and striatum. Specifically, given the number of identified regions, we performed a hierarchical average-linkage clustering algorithm on the between-group connectivity of regions identified across the two interaction maps (see **Online Methods**). Put differently, we examined if different areas from the interaction maps show similar statistical grouping. For the cerebellum analysis, we identified three sets of areas that showed quantitatively similar patterns of dysconnectivity (**Fig. 3b**). The inset shows the distribution of areas in the three sets an axial slice (color-coded green, fuchsia and blue, as in the dendrogram). Next, we characterized the interaction effects for each set of areas produced by the clustering algorithm. Specifically, for a given striatal or cerebellar parcel/seed we averaged connectivity for all areas within a set produced by the clustering algorithm (**Fig. 3c**). We did this separately for both SCZ (red bars) and CON (black bars) groups. Put differently, each of the three sets of areas by definition shows quantitatively similar interaction effects (i.e. they are grouped by the clustering algorithm). The goal here is to characterize how the three sets of areas produced by the clustering algorithm differ. In Set 1, areas exhibited higher mean connectivity in SCZ compared to CON (i.e. hyper-connected on average). In Set 2, areas exhibited lower mean connectivity in SCZ (i.e. hypo-connected on average). The difference between SCZ and CON was less pronounced in Set 3 ROIs and exhibited a 'mixed' motif. Next, we averaged exclusively across sensory (VIS and SOM; pink) and associative (DAN, VAN, LIM, FPCN, DMN; teal) parcels to test if the observed alterations are preferential to higher-order networks. This analysis indicated that the between-group effect in each set is much more pronounced for associative parcels than sensory parcels (**Fig. 3d**). Put simply, the entire source of the *Group* x *Parcels* interaction was driven by a more pronounced associative network alteration in the cerebellum.

Next, we repeated the analyses for the striatal interaction effects. Strikingly, as with the cerebellum, a hierarchical clustering algorithm revealed three sets of areas with similar patterns of connectivity (**Fig. 3f**). The group differences in connectivity in each of these sets driving the striatal interaction effect was similar to those in the cerebellar interaction effect – namely, higher mean connectivity in SCZ than CON for ROIs in Set 1, lower mean connectivity in SCZ than CON for ROIs in Set 2, and a less ostensible difference for ROIs in Set 3 (**Fig. 3g**). These between-group differences were not as pronounced in striatal associative versus sensory parcels than in the analogous cerebellar analysis (**Fig. 3h**) because there was only one sensory parcel in the striatum.

Finally, we computed the statistical similarity of these sets of ROIs between the cerebellum and striatum (**Fig. 4i-k**). Specifically, for each subject, we averaged Fz values across all ROIs in each cerebellar and striatal set. We did so for each parcel within the striatum and the cerebellum (e.g. the FPCN parcel). This revealed a robust and consistent relationship between cerebellar and striatal values across all sets. This strongly supports consistency of interactive effects for cerebellar and striatal ROIs for individual subjects. This relationship held for all networks (Set 1: r=0.455, p<2.20e-16; Set 2: r=0.393, p=2.77e-13; Set 3: r=0.394, p=2.39e-13) and particularly for the FPCN (Set 1: r=0.538, p<2.20e-16; Set 2: r=0.475, p<2.20e16; Set 3: r=0.367, p=1.16e-11; see **Supplementary Fig. S16** for all individual parcels/networks). Collectively, these analyses suggest that interactive brain-wide network disturbances are highly similar between the cerebellum and striatum. However, they are particularly obvious and highly consistent in certain functional networks, especially those involved in higher-order executive tasks.

Figure 3. *Group* x *Parcel* interaction effect for cerebellar and striatal connectivity. Parallel analyses were conducted independently for the cerebellum and striatum, using the functionally-defined 7 cerebellar and 6 striatal parcels. **(a)** Surface view (left) and volume slice view (right) of regions of interest (ROI) revealing a significant *Group* x *Parcel* interaction effect for the cerebellar analysis. Slice outlined in yellow is magnified in inset in panel **b**. **(b)** Each of the 37 cerebellar interaction ROIs were assigned to one of three sets based on the between-group differences in functional connectivity of all 7 cerebellar functional parcels using an average-linkage hierarchical clustering algorithm, such that ROIs within a set share the most similar patterns of group differences in seed-based connectivity. Inset shows location of ROIs color-coded for each set. **(c)** To illustrate the sources of the interaction effect, the mean functional connectivity for each set of ROIs is shown separately for SCZ and CON subjects in each of the cerebellar parcels, averaged across all ROIs in the set. Error bars indicate standard error.

ROIs in Set 1 exhibit higher mean connectivity in patients compared to controls, whereas ROIs in Set 2 exhibit lower mean connectivity in patients. **(d)** This effect is more pronounced for associative parcels (pink) than for sensory parcels (teal). ROIs in Set 3 are less differentiated between patients and controls. **(e-h)** Parallel analysis conducted for the 60 interaction ROIs from 6 striatal functional parcels. **(i-k)** Correlations between mean functional connectivity (Fz) of all cerebellar and striatal parcels in **(i)** Set 1, **(j)** Set 2, and **(k)** Set 3 interaction ROIs, across SCZ and CON subjects. Displayed *r* values are across all subjects (N=320, one outlier removed). Abbreviations: Sens., sensory networks; Assoc., associative networks; VIS, visual network; SOM, somatomotor network; DAN, dorsal attention network; VAN ventral attention network; LIM, limbic network; FPCN, frontoparietal control network; DMN, default mode network.

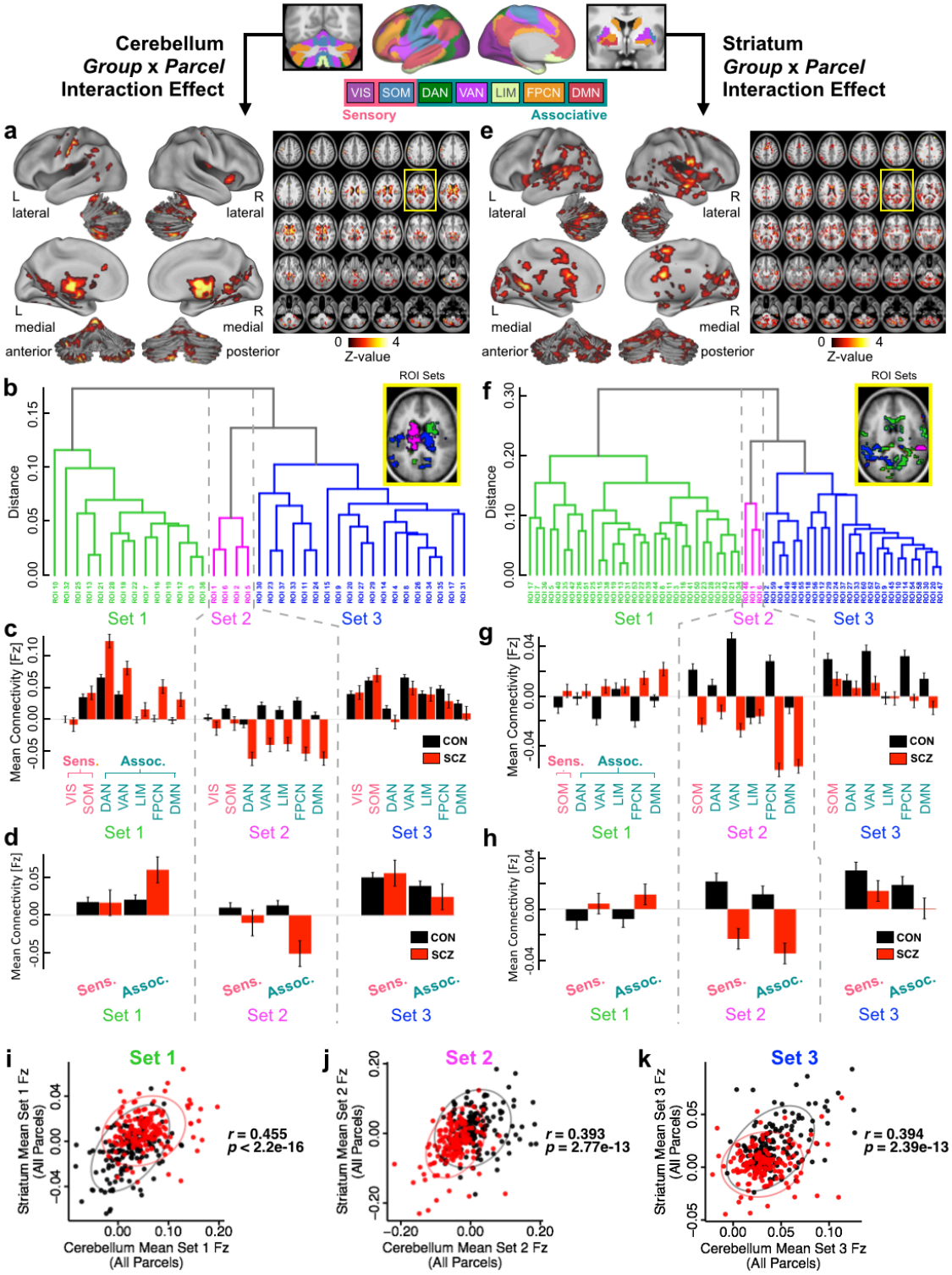

Next, to further establish that the SCZ dysconnectivity was more pronounced in associative than in sensory networks, we examined seed-based functional connectivity maps of each parcel. Qualitatively, the between-group dysconnectivity for associative parcels closely matched the main group dysconnectivity effect (i.e. across all parcels, **Fig. 1b** and **1e**). This was markedly less prominent for sensory parcels across both cerebellum and striatum. To quantitatively verify this, we examined the similarity of the FPCN parcel (**Fig. 4a-b, g-h**) and the SOM parcel between-group effects (**Fig. 4d-e, j-k**) in relation to the main effects across both cerebellum and striatum. Specifically, we correlated unthresholded whole-brain between-group maps for the FPCN parcel with the unthresholded overall dysconnectivity maps (i.e. maps in **Fig. 1b** and **1e**). **Fig. 4c** highlights the similarity between FPCN and overall effects across all parcels (Cerebellum: r=0.914, p<1.0e-15; Striatum: r=0.913, p<1.0e-15). In contrast, the SOM effect dysconnectivity was substantially less similar to the main effects for the cerebellum and striatum (r=0.696, p<1.0e-15; r=0.754, p<1.0e-15). This constituted a highly significant difference between correlations for the FPCN and SOM similarity (Cerebellum: t=-255.12, p<1.0e-15, Striatum: t=-124.43, p<1.0e-15, William's test for dependent correlations). The full expansion of all pair-wise thresholded and unthresholded maps is shown in **Supplementary Fig. S20-S25.** Collectively, these effects buttress prior analyses by showing pervasive disruptions across brain-wide networks that preferentially affect associative functional systems in SCZ.

Relationship Between Hyper-connectivity and Hypo-connectivity Across Individuals. Presented analyses highlight that the alterations are strongly driven by associative networks within the cerebellum and striatum. However, more broadly, it is unknown if the observed hyper-connectivity and hypo-connectivity effects that dominate all presented analyses arise are linked. Alternatively, the bi-directional disruption may result from functionally independent systems-level perturbations. Put differently, distinct groups of subjects could be driving the hyper- vs. hypo- effects across all analyses. To arbitrate between these possibilities, we quantified the connectivity strengths across subjects for areas showing hyper- and hypo-connectivity generally. There was a significant negative relationship between cerebellar hypo-and hyper-connectivity in CON (r=-0.77, p<2.2e-16), indicating that control subjects with the weakest coupling between cerebellar-sensorimotor regions also show the strongest coupling between cerebellar-thalamo-striatal-prefrontal regions (**Fig. 5a**). This effect replicated in the SCZ sample (r=-0.49, p<4.1e-11), but it was significantly attenuated compared to CON (Z=-4.29, p<0.001). Similarly, CON subjects with the weakest striatal-sensorimotor coupling showed the strongest striatal-thalamo-prefrontal-cerebellar coupling (r=-0.85, p<2.2e-16), and an attenuated effect was seen in SCZ subjects (r=-0.67, p<2.2e-16; Z=-3.95, p<0.001; **Fig. 5b**). Additionally, CON subjects that showed the strongest coupling with cerebellum also exhibited the strongest coupling with striatum, for both the hyper-connectivity (r=0.64, p<2.2e-16, **Fig. 5c**) and hypo-connectivity (r=0.75, p<2.2e-16; **Fig. 5d**) effects. This relationship was also present but attenuated in SCZ subjects (hyper-connectivity: r=0.34, p<1.5e-5, Z=3.58, p<0.001; hypo-connectivity: r=0.60, p<2.2e-16, Z=2.48, p=0.013). Note that in all **Fig. 5** panels, SCZ subjects show a diagonal 'shift' relative to CON across both zero-lines (dashed green), suggesting that the differences in hyper- and hypo-connectivity in SCZ may share a source of disturbance. Collectively, these analyses support the hypothesis that perturbations in information flow across these networks may stem from related systems-level phenomena, as opposed to functionally independent perturbations.

Figure 4. Group connectivity differences for associative versus sensory cerebellar and striatal parcels. (a) Surface view of regions for which connectivity with the cerebellar FPCN parcel, an exemplar "associative" parcel, showed significant between-group differences, p<0.05. **(b)** Density plots show distribution of connectivity strength (Fz) values within voxels showing significant hyper- and hypo-connectivity. Bar plots show mean connectivity averaged across all voxels in hyper- and hypo-connected areas. **(c)** Correlation between the voxelwise unthresholded whole-brain group dysconnectivity maps from the cerebellar FPCN parcel and the cerebellar main effect of group. Similar analyses are shown for the **(d-f)** cerebellar SOM parcel, **(g-i)** striatal FPCN parcel, and **(j-l)** striatal SOM parcel. Note the high resemblance between the associative parcel effect and the main effect of group for both the cerebellar and striatal analyses. Contrarily, the sensory parcel effects are significantly less similar (Cerebellum: t=-255.12, p<1.0e-15, Striatum: t=-124.43, p<1.0e-15, William's test for dependent correlations). Abbreviations: FPCN, frontoparietal control network; SOM; somatosensory network.

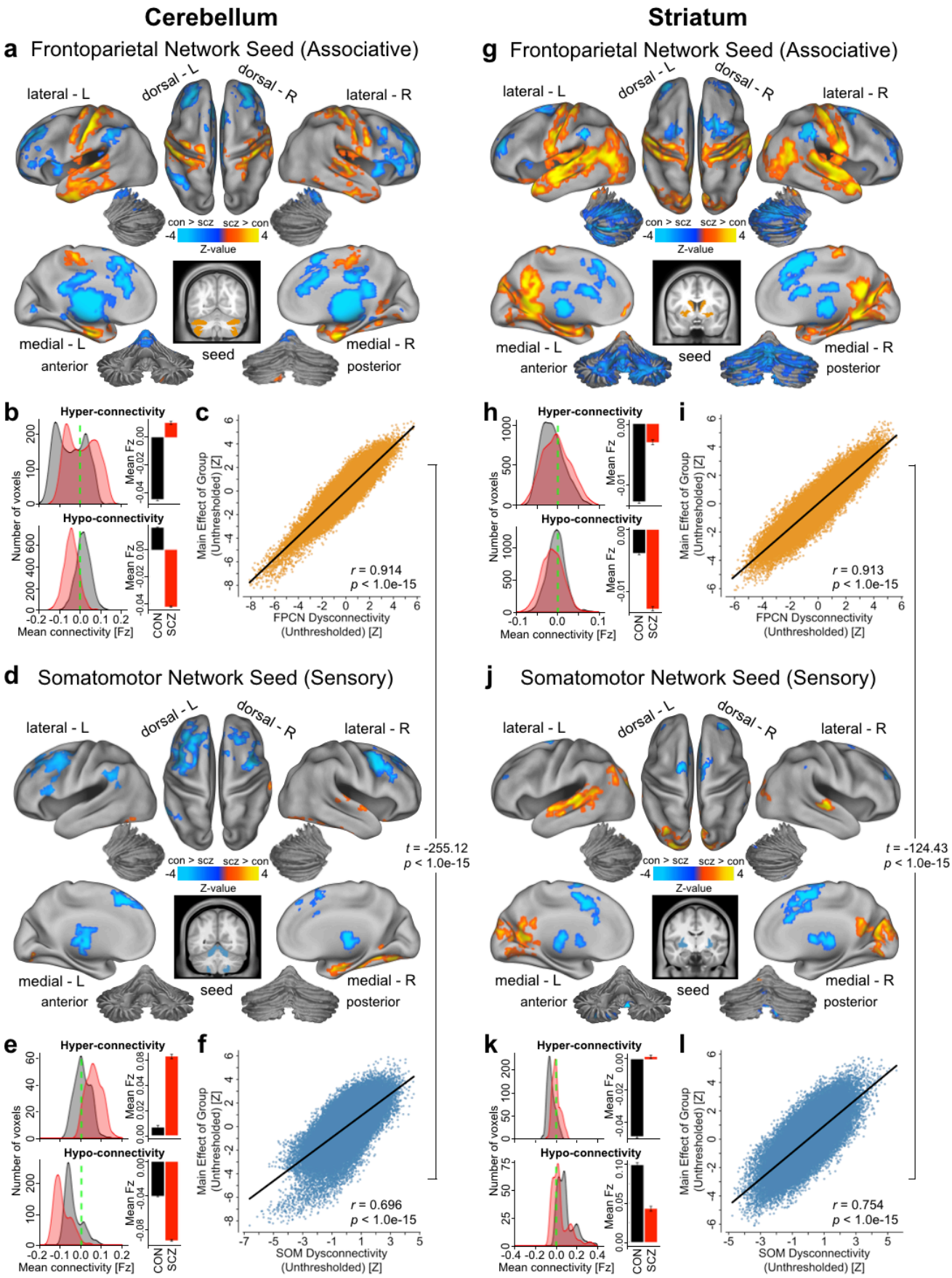
Cerebellum
Striatum
a Frontoparietal Network Seed (Associative)
g Frontoparietal Network Seed (Associative)
lateral - L
dorsal - L
dorsal - R
lateral - R
con > scz
scz > con
-4
4
Z-value
medial - L
medial - R
anterior
posterior
seed
b
Hyper-connectivity
Hypo-connectivity
Number of voxels
Mean Fz
Mean connectivity [Fz]
CON
SCZ
c
Main Effect of Group (Unthresholded) [Z]
FPCN Dysconnectivity (Unthresholded) [Z]
r = 0.914
p < 1.0e-15
h
i
r = 0.913
p < 1.0e-15
d Somatomotor Network Seed (Sensory)
j Somatomotor Network Seed (Sensory)
t = -255.12
p < 1.0e-15
t = -124.43
p < 1.0e-15
e
f
SOM Dysconnectivity (Unthresholded) [Z]
r = 0.696
p < 1.0e-15
k
l
r = 0.754
p < 1.0e-15

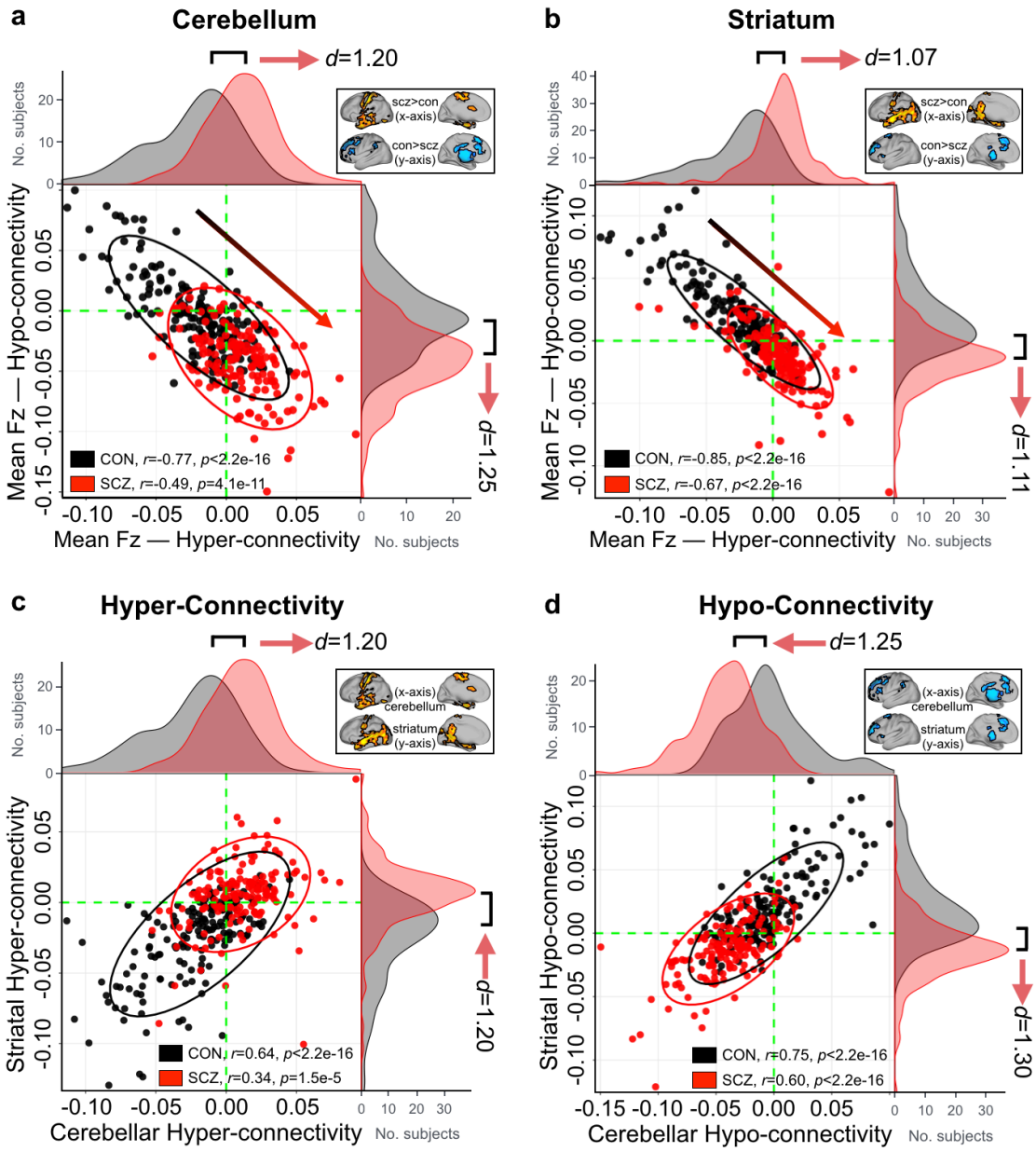

Figure 5. Relationship between cerebellar and striatal hyper- and hypo-connectivity across subjects. (a) Significant negative relationship evident between average hyper- and hypo- whole-brain connectivity with the cerebellum across all CON (black data points). SCZ (red data points) showed a 'shift' across the zero lines, indicating weaker prefrontal-striatal-thalamic-cerebellar coupling but stronger somatomotor-cerebellar coupling. Ellipses for each group mark the 95% confidence intervals. Distributions of average connection strengths for each subject show a shift in cerebellar coupling in SCZ, highlighting increased cerebellar coupling with somatomotor regions and decreased coupling with prefrontal-striatal and thalamic regions for patients. Inset shows regions of hyper- and hypo-connectivity with the cerebellum in SCZ, from **Fig. 1b. (b)** A similar effect is seen in an independently conducted analysis on whole-brain striatal connectivity. Again, SCZ showed a shift across the zero lines relative to CON, suggesting that the differences in hyper- and hypo-connectivity observed in SCZ may share a source of disturbance. Inset shows regions of hyper- and hypo-connectivity with the striatum in SCZ, from **Fig. 1e**. **(c)** CON subjects with the highest cerebellar connectivity in hyper-connected regions also show highest connectivity in striatal hyper-connected regions. Shift in SCZ subjects relative to CON is evident for both cerebellar and striatal hyper-connectivity (identical data as those plotted along X-axes in panels **a** and **b**), suggesting the underlying disruption is linked across these two systems. **(d)** Similarly, SCZ subjects show a shift in both cerebellar and striatal hypo-connectivity.

Data-Driven Clustering of Cerebellar and Striatal Dysconnectivity. While robust, all presented analyses have used *a priori* functional networks to reveal shared CSTC perturbations in SCZ. However, there may be important functional differences in the spatial distribution of these network parcels in patients. In other words, patients may not show a clean separation that is assumed to be present in controls of cerebellum and striatum networks. Therefore, to test if the effects hold without *a priori* network assumptions, we performed data-driven *k*-means clustering on voxelwise group dysconnectivity for both the cerebellum and the striatum (see **Online Methods** and **Supplementary Fig. S26** for details). If the hypothesized *a priori* disruptions are indeed intrinsic and not attributable to spatial network assumptions, then the results should replicate via data-driven between-group parcellation of the cerebellum and striatum. We report several cluster solutions of between-group differences (see **Supplementary Fig. S27** for full 4-, 6- and 7-cluster solutions). While the pattern is highly similar irrespective of cluster choices, here we highlight the 7-cluster solution for the cerebellum and the 6-cluster solution for the striatum to allow a direct comparison with the *a priori* network parcellation granularity (i.e. this was the number of networks in the *a priori* parcellations).

The clustering solution for the cerebellum revealed well-defined and bilaterally symmetrical clusters, which is not consistent with the effects being driven by artifact (**Fig. 6a**). A voxelwise measure of dissimilarity (1-eta^2; see **Online Methods**) shows regions with the numerically greatest degree of dysconnectivity between SCZ and CON. These foci were also bilaterally symmetrical (**Fig. 6b**). Next, we tested if these data-driven clustering solutions map onto the *a priori* network parcel results. Here we quantified the relationship between the group dysconnectivity for each of the obtained clusters and each *a priori* cerebellar parcel (top 7 rows) as well as the average across all parcels (bottom row). This yields a 8x7 matrix of Pearson's *r* values shown in **Fig. 6c**, where the columns of the matrix are ordered such that the trace of the parcel-by-cluster square matrix is maximized. As illustrated by the diagonal, there was a selective mapping between data-driven and *a priori* dysconnectivity patterns. Notably, six of the 7 clusters have their strongest correlation value along the diagonal, suggesting that these clusters mapped selectively to existing parcels. This selective mapping can also be seen with the alternative k=4 and k=6 cluster solutions (**Supplementary Fig. 37**). Collectively, this indicates qualitatively similar disruptions irrespective of analytic methods used to define cerebellar dysconnectivity in SCZ. This is corroborated, for instance, by examining Cluster 4 (**Fig. 6a**, bright green), which is most similar in dysconnectivity to the associative parcels (r=0.81, p<0.001, **Fig. 6d**), indicating that in the context of SCZ-related disturbances it exhibits a functionally 'associative-like' profile. We show the threshold-free between-group differences in whole-brain connectivity of this 'associative-like' cerebellar cluster in **Fig. 6e** (see **Supplementary Fig. S28-S30** for maps of all clusters for 4, 6, and 7-cluster solutions).

Importantly, *k*-means clustering with k=6 on striatal voxelwise dysconnectivity yielded a consistent and bilaterally symmetrical solution (**Fig. 6f**). The most dissimilar voxels are again indicated in bright yellow in **Fig. 6g,** suggesting a non-uniform pattern of striatal alterations. As with the cerebellum, there was a selective mapping between data-driven and *a priori* dysconnectivity patterns for the striatum (**Fig. 6h**). Cluster 3 (**Fig. 6f**, bright green) exhibited a pattern of dysconnectivity most similar to those of associative functional parcels (r=0.81, p<0.001, **Fig. 6i**). Finally, threshold-free between-group differences in whole-brain connectivity of this 'associative-like' striatal cluster highlight a pattern that in line with the *a priori* association parcel analysis (**Fig. 6j**, see **Supplementary Fig. S31-S33** for maps of all clusters for 4, 6, and 7-cluster solutions). Additionally, we report the same data-driven clustering solutions for cerebellum and striatum in CON only (**Supplementary Fig. S36**), which fully replicated the functional parcels identified previously by Bucker et al. and Choi et al.[2, 3].

Figure 6. Voxelwise clustering of cerebellar and striatal group difference in connectivity. (a) Results for *k*-means 7-cluster solution identifying cerebellar voxels with the most similar patterns of between-group connectivity differences. Note the cluster solution is highly symmetrical (blue arrows). **(b)** Cerebellar dysconnectivity based on group dissimilarity. Brightest voxels indicate greatest between-group differences. **(c)** Matrix of correlations (Pearson's *r*) between dysconnectivity of obtained clusters and dysconnectivity of functional parcels. Cluster numbers (column headings) are colored as in **a**. Functional parcels (row headings) are labeled and colored as in **Figure 1a** and original parcellation[1]. Columns have been ordered such that the trace of the parcel-by-cluster square matrix is maximal among all permutations. Cluster-seeded dysconnectivity shows a range of correlation strengths with functional parcel-seeded dysconnectivity. Cluster 4 (bright green) is strongly correlated with

associative parcels, as well as with the overall main effect of group, suggesting that it is a functionally 'associative-like' cluster. **(d)** Scatterplot showing high degree of correlation between voxelwise whole-brain group dysconnectivity (Fz values) of cerebellar cluster 4 (the 'associative' cluster) and voxelwise whole-brain group dysconnectivity (Fz values) across all cerebellum parcels. **(e)** Surface unthresholded Z-maps showing between-group connectivity for cerebellar executive cluster (shown in inset). **(f-j)** Identical analyses conducted independently for between-group differences in whole-brain striatal connectivity. Striatal cluster 3 (bright green) is strongly correlated with associative parcels, as well as with the overall main effect of group, suggesting that it is a functionally 'associative-like' cluster.

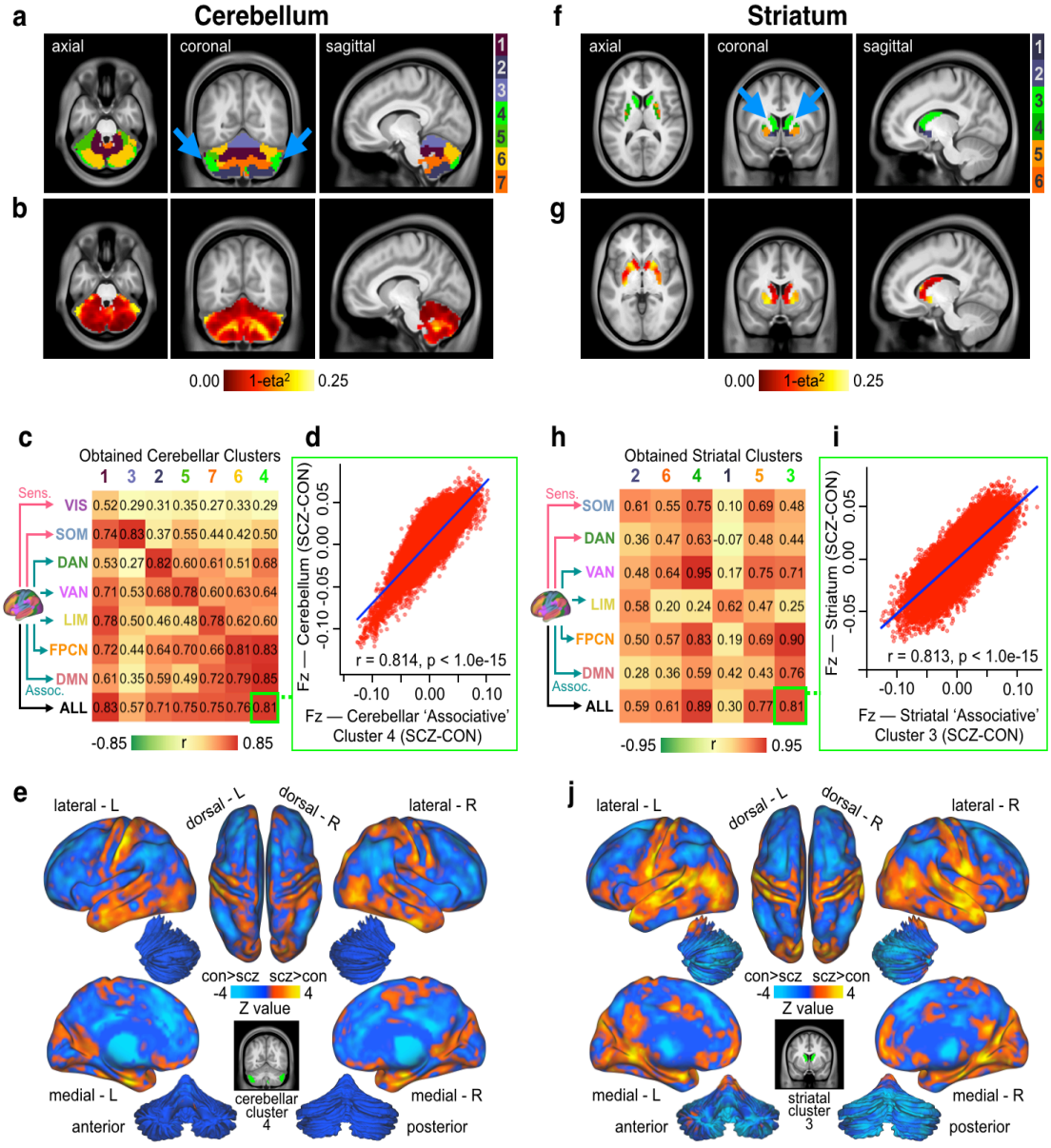

Cerebellar and Striatal Dysconnectivity Features Predict Diagnostic Group Status. Above, we show consistent and robust alterations in BOLD functional relationships across striatal and cerebellar functional subdivisions in SCZ. Next, we examined if these effects may yield a sensitive and specific binary classification of diagnostic group status. Specifically, we used a support vector machine (SVM) binary classifier to test if cerebellar and striatal parcel connectivity features reliably distinguish between groups. In turn, we tested three secondary questions related to the brain-wide patterns of disruptions: First, we tested if any of the identified features selectively 'drive' the classification performance or if the classifier performance remains

stable irrespective of parcel feature used. Put differently, if SCZ is associated with brain-wide alterations across CSTC systems, then cerebellar and striatal parcel features should yield comparable classification performance, as there should be overlap in the disruptions. Second, a corollary of this hypothesis is that specific parcels within the striatum or cerebellum may drive classifier performance. In particular, given that our previous analyses show preferential SCZ disruptions in associative parcels, we hypothesized that associative parcel features would yield the highest classification performance. However, if the brain-wide disruptions are shared across CSTC systems, then the same network parcels should contribute information to the classifier irrespective of whether they are selected from the striatum or the cerebellum. Third, we examined whether classifier performance could be improved by combining select subsets of cerebellar and striatal parcel features. We hypothesized that if there exists considerable overlap in diagnostically relevant information across cerebellar and striatal parcels, a classifier using a combination of all parcel features would not markedly outperform the most discriminatory single-feature classifier. Alternatively, a multi-feature classifier would yield better performance if interactive effects across specific cerebellar and striatal parcel features contribute unique diagnostically relevant variance.

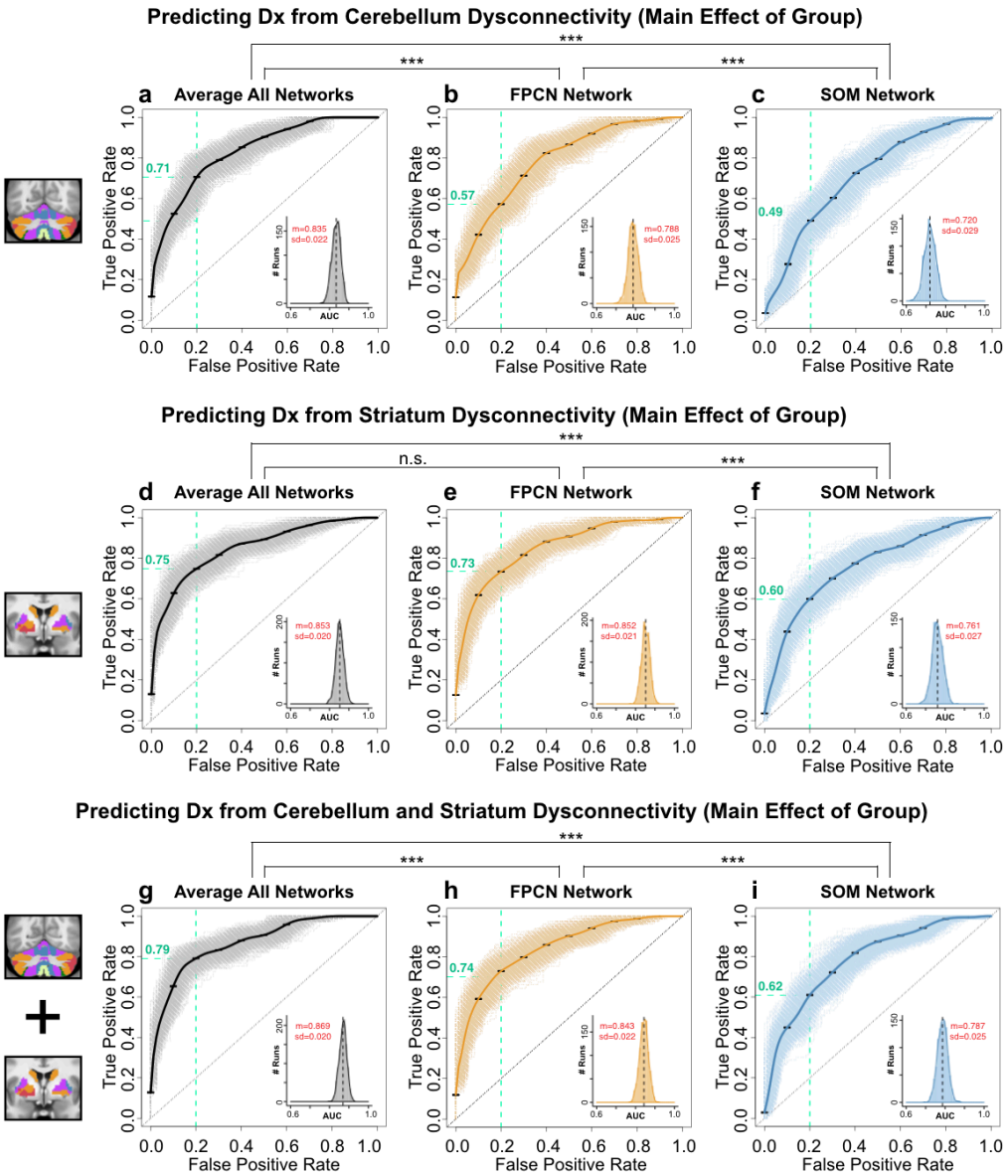

Figure 7. Receiver operating characteristic (ROC) curves from binary classifiers of diagnostic status trained on cerebellar and striatal dysconnectivity features. Exemplar associative (FPCN) and sensory (SOM)

parcels, as well as the average combined across all parcels (AVERAGE), are shown. **(a)** Performance of classifier using AVERAGE dysconnectivity across all cerebellar parcels. Bold black curve plots the mean true positive rate (TPR) at each false positive rate (FPR) across 1,000 cross-validation runs (standard error bars shown in black). Grey curves show individual results from all cross-validation runs. Inset plots the distribution of the Area Under the Curve (AUC) for all 1,000 runs; black dashed line shows the mean AUC. Mean (m) and standard deviation (sd) of the AUC distribution are displayed in red. **(b)** Performance of classifier using cerebellar FPCN dysconnectivity. **(c)** Performance of classifier trained using cerebellar SOM parcel dysconnectivity. Green dashed lines show the TPR for each classifier at FPR=0.20. The cerebellar FPCN TPR=0.71, indicating that this classifier achieves a higher sensitivity than the SOM classifier (TPR=0.49) at the same 'cost' of specificity. Similarly, the AUC performance is significantly higher for the FPCN than the SOM classifier (t=55.692, df=1953.4, p<1.0e-15). Asterisks denote significance at p<0.001 in a two-tailed t-test between the indicated AUC distributions. **(d-f)** Performance of classifiers using striatal AVERAGE, SOM, and FPCN features. Again, the FPCN classifier outperformed the SOM classifier, as indicated by sensitivity at FPR=0.20 (FPCN TPR=0.73, SOM TPR=0.60) and AUC (t=83.869, df=1871.2, p<1.0e-15). **(g-i)** Performance of classifiers using combined cerebellar and striatal AVERAGE, FPCN, and SOM features. See **Supplementary Fig. S38-S40** for ROC curves of all parcels.

First, to test if cerebellar and striatal feature are comparable for classification, we used the connectivity strengths (Fz values) of hyper- and hypo-connected areas from each of the seed-based functional connectivity analyses as input features. Each classifier was trained on a randomly selected subset (50%) of subjects and tested on the remaining subjects, repeated 1,000 times (cross-validation runs, see **Online Methods**). Classifier performance across specific exemplar parcel features is shown in **Fig. 7** (see **Supplementary Fig. S38-S40** for all classifiers). Cerebellar and striatal classifiers yielded highly comparable performance, supporting the hypothesis of shared brain-wide disruptions across both the cerebellum and striatum. Specifically, the classifier trained on the average dysconnectivity across all parcels (AVERAGE) was similar for the cerebellum (accuracy=75.0%, sensitivity=76.9% & specificity=73.2%, mean area under the receiver operating characteristic curve (AUC)=0.835, **Fig. 7a**) and the striatum (accuracy=75.7%, sensitivity=79.0% & specificity=72.5%, AUC=0.853, **Fig. 7d**). Collectively, these measures suggest that the cerebellum and striatum may exhibit shared disruptions. Consequently, cerebellum and striatum do not outperform one another.

As noted, our second classifier hypothesis was to test if disruptions in SCZ are more pronounced in associative parcels relative to other parcels within cerebellar and striatal systems. This would result in better performance for classifiers trained on associative parcel features relative to sensory parcel features. Both the cerebellar and striatal FPCN classifiers outperformed the SOM classifiers (Cerebellum-FPCN Classifier: accuracy=71.2%, sensitivity=80.6% & specificity=61.8%, AUC=0.788, **Fig. 7b**; Striatum-FPCN Classifier: accuracy=75.7%, sensitivity=71.3% & specificity=71.0%, AUC=0.852, **Fig. 7e**; Cerebellum-SOM Classifier: accuracy=66.1%, sensitivity=76.9% & specificity=61.0%, AUC=0.720, **Fig. 7c**; Striatum-SOM Classifier: accuracy=68.3%, sensitivity=77.1% & specificity=59.7%, AUC=0.761, **Fig. 7f**). This was supported by a formal test of differences in FPCN vs. SOM AUC parameters across the cerebellum (t=55.692, df=1953.4, p<1.0e-15) and striatum (t=83.869, df=1871.2, p<1.0e-15). This result is consistent with the hypothesis of shared CSTC disruptions being preferential to associative parcels in SCZ.

In turn, our third classifier hypothesis tested if combining cerebellar and striatal information would improve classifier performance relative to the single best feature. We first trained classifiers on a linear combination of both cerebellar and striatal parcel features (referred to as "combined" classifiers below). The combined AVERAGE classifier yielded the highest performance (mean accuracy of 78.7%, with 80.7% sensitivity and 76.7% specificity, AUC=0.869, **Fig. 7g**). This was comparable to the combined FPCN classifier (accuracy=74.2%, sensitivity=80.8%, specificity=67.6%, AUC=0.843, **Fig. 7h**). Again, the combined classifier trained with SOM yielded the lowest performance (accuracy=70.8%, sensitivity=75.7%, specificity=66.0%, AUC=0.787, **Fig. 7i**). We then examined if interactive effects between these striatal and cerebellar parcel features contribute information that improves classification. Here we trained a 13-feature classifier using connectivity from all 7 cerebellar and 6 striatal parcels as predictors. This multi-feature classifier did not perform better than the classifiers trained on one parcel feature per subject (accuracy=77.3%, sensitivity=78.6% & specificity=76.0%, AUC=0.859, **Fig. 8a**), suggesting that interactions between parcel

features did not contribute unique additional information. In further support of this effect, no added number of additional features appreciably improved classifier performance compared to the classifier trained on the single most discriminatory feature (**Fig. 8b**). Additionally, the relationship between the AUC of individual features and the weight assigned to them in the multi-feature classifier was not significant, suggesting that no informational tradeoffs were made by selecting certain parcel features over others in the 13 multi-feature classifier (**Fig. 8c**; all features: r=0.420, p=0.153, dashed grey line; excluding most discriminatory feature: r=0.11, p=0.74, blue line). Lastly, classifier performance was not improved by including the interactions between the two most strongly weighted parcel features – namely cerebellar and striatal FPCN and DAN – as additional predictors (accuracy=77.1%, sensitivity=79.1% & specificity=75.1%, AUC=0.856, **Fig. 8d**). Importantly, the classifier was not driven by group differences in head motion or SNR (**Supplementary Fig. 41**). These analyses suggest that diagnostically informative patterns are highly shared across cerebellar and striatal features, and no additional information is contributed by their interactions across these analyses.

Collectively, we show that SVM binary classifiers using cerebellar and striatal connectivity features can distinguish between groups with high sensitivity and specificity. These classifier results are consistent with prior analyses indicating that neither cerebellum nor striatum as a whole drives classifier performance, suggesting that network disruptions in SCZ persists across both systems. Furthermore, associative parcels in both cerebellum and striatum are particularly discriminatory between groups, supporting both *a priori* and data-driven results presented above. Put differently, brain-wide disturbance in SCZ appear most pronounced for higher-order associative subdivisions across cerebellar and striatal functional parcels.

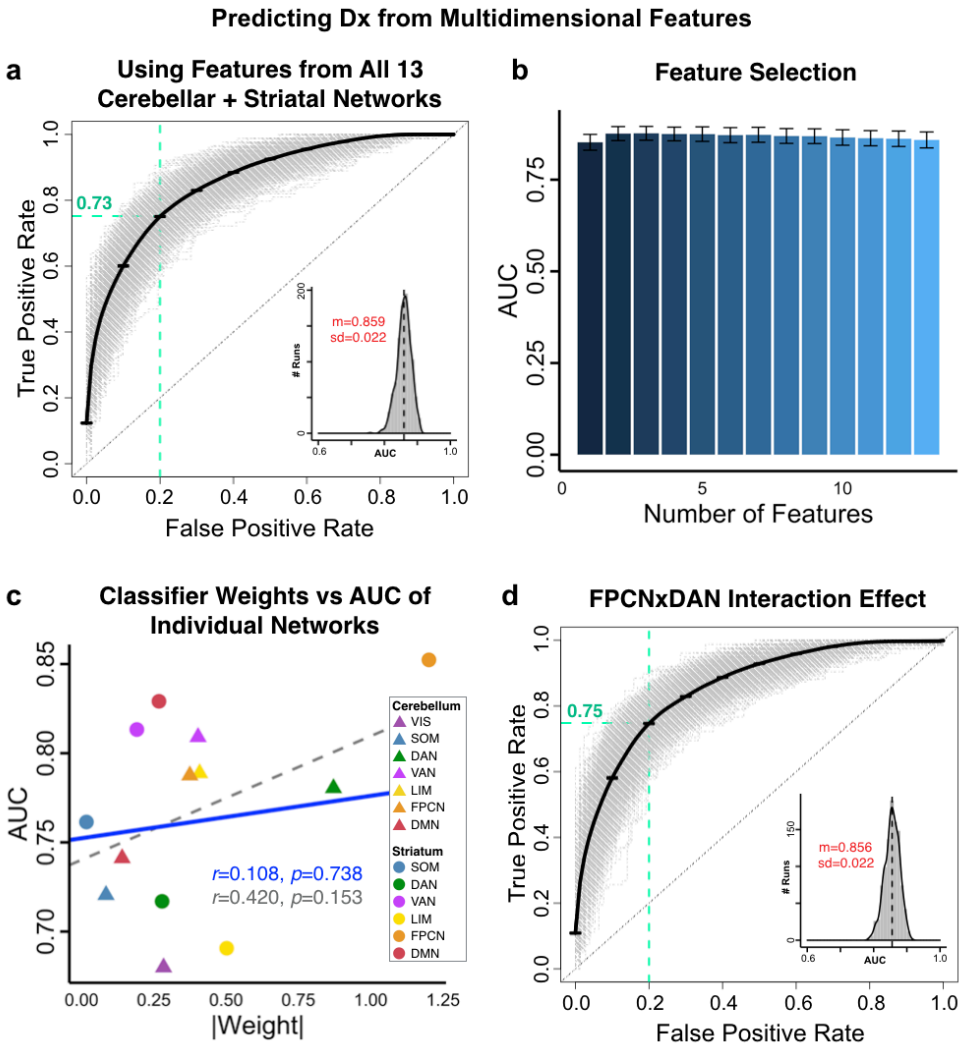

Figure 8. Binary classifiers using multidimensional predictors. (a) We trained a linear kernel SVM to distinguish between SCZ and CON subjects using connectivity features from all 7 cerebellar and 6 striatal parcels, in a 13-dimensional feature space. This multi-feature classifier did not perform significantly better than classifiers trained on individual features (**Fig. 7**, **Supplementary Fig. S38-S40**). ROC curves show the TPR plotted against the FPR of the classifier trained on all 13 parcel features. Grey curves show ROC curves for 1,000 individual cross-validation runs; bold black curve shows mean ROC curve (standard error bars in black). Green dashed lines indicate TPR=0.73 at FPR=0.20. Inset shows the distribution of the AUC across all 1,000 runs (black dashed line shows mean), with mean AUC (m) and standard deviation (sd) displayed in red. **(b)** Comparison of AUC performance across classifiers with 1 through 13 features. There were no significance differences in AUC between any of these classifiers, indicating that no additional number of features improved performance compared to the classifier trained on the single most discriminatory feature. Bar plots show the mean AUC of each classifier; error bars show standard deviation. **(c)** Plotting the mean AUC from classifiers trained on each individual parcel feature (from **Supplementary Fig. S38-S39**) against the absolute weight of these parcels in the 13-feature classifier shows that there is no linear dependence between the two. Dashed grey line shows correlation between all points (r=0.42, p=0.15); solid blue line shows correlation between all points excluding the striatal FPCN, the most discriminatory feature (r=0.11, p=0.74). **(d)** ROC curves of a classifier trained with interaction effects between the two strongest-weighted seeds. In addition to the individual parcel features, we added the four-way interaction between the cerebellar FPCN and DAN and the striatal FPCN and DAN as features. Again, the classifier performance was not improved, indicating that no additional information is contributed by the interactive effect.

DISCUSSION

Identifying robust, replicable and neurobiologically-grounded neuroimaging markers for neuropsychiatric illness in general and SCZ in particular remains a major knowledge gap and an obstacle for rational treatment development. An ongoing theoretical debate, particularly relevant for biomarker development in SCZ, concerns a tension between hypotheses suggesting that SCZ neural disturbances manifest across large-scale functional networks (i.e. brain-wide) and hypotheses suggesting they occur in select regions (i.e. 'hotspots' of disturbance)[30]. Resolving this tension is critical to informing biomarker development that can guide rational treatment for either targeted neuropathology in specific areas or diffuse alterations that span brain-wide pathways. Put simply, do we develop treatments that target dysconnectivity somewhere or everywhere? Here we show that the cerebellum and the striatum, both part of the large-scale functional neural circuitry, exhibit highly similar bi-directional whole-brain alterations characterized by hyper-connectivity with sensorimotor cortex and hypo-connectivity with prefrontal cortex (PFC) and thalamus in patients with SCZ. Furthermore, these alterations are more pronounced in higher-order associative areas than in sensory areas throughout both cerebellum and striatum. The perturbations underlying the hyper- and hypo-connectivity are related across both patients and healthy controls. Additionally, using a complementary data-driven approach, we demonstrate that the cerebellum and striatum could be divided into functionally distinct disrupted circuits. Finally, we demonstrate, using SVM-based machine learning, that 'core' associative alterations cut across both cerebellum and striatum and drive diagnostic classification. Collectively, these data are consistent with pervasive brain-wide bi-directional alterations in cortico-striato-cerebellar circuits in SCZ that manifest most severely across associative networks.

Brain-wide Disruptions Occur Across CSTC Functional Circuits in SCZ. Numerous lines of evidence and theoretical hypotheses implicate localized regional disruptions in SCZ. For instance, the dopamine hypothesis of SCZ strongly points to a striatal disruption in DA signaling. This is supported by the clinical potency of first-generation antipsychotics (and to some extent, second-generation "atypical"[31]), whereby blockade of striatal dopamine D2 receptors correlates with therapeutic efficacy for psychotic symptoms[32, 33]. In humans, these receptors are primarily expressed in the dorsal striatum[34-36]. Complementary work centered on the DA hypothesis implicates hippocampal, thalamic and focal ventral tegmental area (VTA) alterations as central in the formation of positive symptoms of SCZ[37, 38].

In contrast, glutamatergic hypotheses of SCZ, such as the prominent NMDAR hypo-function model, generally suggest a more widespread disruption centered on cortical microcircuits[39, 40]. Behaviorally, the SCZ

spectrum is associated with broad deficits, including impaired executive cognitive functioning, deficits in perception, belief formation, as well as severe affective deficits marked by amotivation and anhedonia[26, 41-45]. Collectively, it has been challenging to link such a broad-ranging behavioral disturbances across the SCZ spectrum to a single or a few brain regions.

To date, neuroimaging studies have provided support for both 'local hotspot' and 'widespread' alterations, largely as a consequence of analytic method used. For instance, the thalamus has featured prominently in theoretical models of SCZ, both as a region of core putative disruption and part of a broader dysfunctional cortico-striato-thalamic loop. Interestingly, several replications have confirmed bi-directional perturbations in functional coupling of the thalamus with cortex in SCZ, whereby patients exhibit increased thalamo-somatomotor cortex but decreased thalamo-prefrontal cortex coupling[11, 12]. However, even these thalamic dysconnectivity findings could not explicitly arbitrate 'local hotspot' versus widespread source of disruptions because the thalamus has been identified as both a core locus of disturbance in SCZ and represents a widely connected relay with the rest of the brain.

Examining if such perturbations manifest across neural systems, or if they are localized to select regions, necessitates the consideration of large-scale brain-wide systems. Here we leveraged existing findings in healthy individuals that have identified large-scale functional networks traversing the cerebral cortex, basal ganglia, and cerebellum[1-3]. If SCZ involves synaptic alterations that are not exclusive to the thalamus, but rather affect distributed neural circuitry, then the bi-directional dysconnectivity seen with the thalamus may also be present across other systems as a shared pattern of disruption, including the striatum and cerebellum.

Presented results, combining complimentary analytic approaches, revealed that bi-directional disruptions in SCZ are indeed present across both the striatum and cerebellum. Moreover, these alterations are particularly pronounced along associative higher-order functional subdivisions of these two systems. Importantly, these data converge across independent analyses, which included functional connectivity conducted via *a priori* subcortical network parcel seeds, voxelwise clustering of dysconnectivity, and binary classifiers of group status that used parcel dysconnectivity features. These three complementary results point to robust bi-directional alterations across both the striatum and cerebellum. Indeed, numerous studies have reported abnormal striatal and cerebellar connectivity in smaller samples of SCZ subjects[16, 18-21, 46, 47], as well as in related psychiatric disorders[48-54]. Our results support and extend these findings, providing evidence for shared perturbations in SCZ across brain-wide systems, in a large cohort of patients and matched controls.

Importantly, while these results strongly indicate that disruptions in SCZ are pervasive across cerebellar and striatal systems, they do not rule out the possibility that these disturbances emerge over time as a consequence of a local 'hotspot' of disruption. Testing this will require careful prospective longitudinal clinical design that starts from the illness prodrome and examines if specific regional markers of dysfunction yield superior prospective classifier performance that also predict the severity of these findings.

Striatal and Cerebellar Disruptions in SCZ. The key purpose of collectively studying the striatum and cerebellum was to test if hypothesized disturbances in SCZ are indeed broadly distributed. The choice of striatal parcels is driven by the well-established observation that striatum shares dense monosynaptic connections with the cortex and thalamus, forming structural cortico-striato-thalamo-cortical loops[55]. In contrast, it is also well established that there are no direct anatomical tracts between the cerebellum and the cerebral cortex, striatum or thalamus[56]. Thus, the choice of the cerebellum is immediately less obvious from an anatomical perspective. However, an important property of evaluating 'functional connectivity' is that coupled BOLD signals do not depend solely on monosynaptic anatomical connections. Indeed, multiple lines of evidence have demonstrated that the cerebellum is a key component of large-scale functional circuits with striatum, thalamus and cortex[1-3]. Trans-synaptic viral tracers have also shown that the cerebellum projects densely to distributed areas of the brain through polysynaptic pathways, and in turn receives extensive polysynaptic projections from the basal ganglia, thalamus and cortex[57]. Consequently, the cerebellum is highly functionally coupled and shares information densely with cortical, striatal and thalamic systems. This is further supported by the presence of functional cerebellar subdivisions that reliably topographically map onto cortical networks[2], albeit through polysynaptic connections. Indeed, Buckner and colleagues found that the proportion of the cerebellum dedicated to each functional network is roughly equivalent to the proportion in the cerebral

cortex, with a majority of cerebellar grey matter being assigned to associative functions. Additionally, numerous studies have demonstrated the involvement of the cerebellum in cognitive and executive functions, establishing that its functionality extends beyond motor coordination[19, 58-62]. Therefore, the inclusion of the cerebellum allows for testing if the observed effect is solely dependent on disrupted direct anatomical connections surrounding structural cortico-striatal-thalamic loops. Collectively, results indicate similar cerebellar and striatal dysconnectivity in SCZ, which appears to be present across the brain. While it remains to be determined if the cerebellar and striatal alterations reflect causes, consequences or compensations, forthcoming models of brain-wide disturbances in SCZ needs to encompass a broader CSTC picture that moves beyond the 'local hotspot' vs. global tension.

Treatment and Diagnostic Implications of Preferential Associative Disturbances Across CSTC. While SCZ patients exhibited changes across both striatum and cerebellum, the associative higher-order subdivisions across both the cerebellum and striatum exhibited the most robust disturbances. Put differently, the observed dysconnectivity in SCZ is strongest along higher-order associative networks within both the cerebellum and striatum, very much in line with prior studies focused on thalamic and cortical networks[11, 12, 28, 63, 64]. This preferentially more severe associative disruption may reflect pervasive brain-wide disruptions in synaptic communication at the level of local microcircuits (e.g. NMDAR dysfunction), which in turn affects the most 'vulnerable' circuits (i.e. associative cortex). Indeed, recent biophysically-informed computational modeling work showed that widespread cellular-level glutamatergic deficits can yield preferentially more severe associative network dysconnectivity. This held when pre-existing higher recurrent excitation in associative (versus sensory) cortex was considered in the model[4, 65, 66]. Such differences in neuronal structure and functional coupling may extend throughout CSTC systems and may underlie the preferentially associative patterns of dysconnectivity observed across the cerebellum and striatum.

Critically, these findings present a challenge for future rational treatment design. As noted, the observed disturbances could arise locally and spread longitudinally to many systems due to the inherent nature of neural functional feedback loops. Alternatively, the may occur pervasively in the first place. Either way, there appear to be some final converging regional expression of more severe dysconnectivity in association networks across cortex, thalamus, striatum and cerebellum. This situation opens up three questions for rational treatment development: do the compensations need to occur somewhere (i.e. hotspot of disturbance if it indeed exists or emergent associative cortex disruption), anywhere (i.e. at any point of the affected CSTC circuit) or everywhere (i.e. global tuning of excitation/inhibition balance across all circuits)? More concretely, these data may imply that designing therapeutic targets for cerebellar circuits may be indicated for SCZ. However, what if indeed the primary locus of pathology involves D2 receptors and thalamo-hippocampal-striatal loops? Then, even though this finding implicates the cerebellum in the 'end-stage' of illness, it may not be a viable initial treatment target (as it represents a consequence). A productive way to address this question is to carefully and longitudinally study duration-of-untreated psychosis (DUP) in early-course illness as a predictor of currently reported CSTC alterations and to map the neurobiology of at-risk clinical populations.

Implications for Development of SCZ Imaging Markers and Rational Treatment Design. These results demonstrate the importance of considering brain-wide disruptions in CSTC functional coupling in characterizing chronic SCZ. Although the presented classifiers were able to leverage cerebellar and striatal parcel features to achieve high group classification accuracy (comparable to other classifiers in the literature[67-71]), there are key considerations that need to be addressed to improve the clinical applicability of neuroimaging biomarkers for SCZ. First, the observed dysconnectivity effects did not relate to state-like measures of positive symptom severity, across several very well powered analyses for both the cerebellum and the striatum. Critically, this modest symptom effect was observed in the context of highly robust individual differences in hyper-/hypo-connectivity relationships across both the cerebellum and the striatum (see **Fig. 5**). This strongly suggests that the reported dysconnectivity may reflect more stable, trait-like markers of disease, at least when analyzed in aggregate. Although the patients we studies did not have comprehensive data for trait-like markers such as cognitive deficits, it is conceivable that the in functional coupling of key neural regions in CSTC circuits reflect differences in stable clinically-relevant behavioral traits, such as cognition. Characterizing the mapping

between functional neural patterns and behavioral measures will be crucial to developing robust, reliable neurobiologically-grounded biomarkers of disease that concurrently map onto behavioral dimensions. Put differently, the purpose of the presented classifier analyses was to explicitly test if cerebellar or striatal systems provide unique information for categorical single-subject classification. They were not, however, optimized for mapping of dimensional behavioral variation in symptoms. Forthcoming studies should test if all information from the identified CSTC dysconnectivity drive stable categorical diagnostic features or if any of the reported features capture dimensional variation in state-like symptoms. Again, to address such questions definitively careful prospective longitudinal clinical studies starting with prodromal stages of illness are needed.

Another key outstanding question concerns whether this observed dysconnectivity is consistent across different psychiatric disorders, or if there are clear patterns that differentiate subgroups of individuals. Earlier results have shown that patients with bipolar disorder exhibit similar, but attenuated, bidirectional patterns of disruption in whole-brain thalamic dysconnectivity[12], with some critical unique features. Studying dysconnectivity across CSTC systems using carefully matched cross-diagnostic samples may reveal similarly shared patterns of bi-directional disruption in patients with a psychiatric diagnosis compared to unaffected individuals. Alternatively, differences in dysconnectivity may emerge cleanly between different diagnostic groups, in a manner that maps on to current DSM categories. On the other hand, it is possible that a population study will reveal patterns of dysconnectivity associated with specific behavioral markers that transcend current categorical boundaries, and would inform an Research Domain Criteria (RDoC)-like dimensional approach to psychiatric classification[72].

Lastly, as noted, a key objective of this study was to test if cerebellar or striatal systems provide unique information for categorical single-subject classification. Here we used BOLD functional connectivity as the only dependent measure, showing that there are no major informational tradeoffs across the cerebellum or striatum. Instead, the classifier performed best when aggregating information across associative networks across both systems. However, classifier accuracy could be improved by integrating information across multiple modalities that can map CSTC systems[71], such as diffusion-weighted imaging (DWI). While each technique faces limitations, the product of BOLD-DWI multimodal neuroimaging has the opportunity to be greater than the sum of its parts as it carries unique sources of information. Therefore, leveraging neuroimaging information across diffusion-weighted, functional, and structural neuroimaging modalities may critically improve the accuracy and generalizability of clinical classifiers.

Conclusion. The field of SCZ research faces a tension between models proposing ‘focal hotspot’ disturbances affecting neural communication versus pervasive alterations that span most neural circuits. The objective was to demonstrate that bi-directional disruptions in functional coupling are robust and highly conserved across both cerebellar and striatal systems of CSTC functional circuits. This shared and pervasive CSTC dysconnectivity in SCZ rules out the possibility of exclusive ‘localized’ thalamic disruptions, at least in chronic states. Instead, results show pervasive brain-wide dysconnectivity that is consistently most pronounced along associative subdivisions of the CSTC networks. Collectively, convergent results using multiple analytic approaches implicate a diffuse neuropathology along the SCZ spectrum, which preferentially affects higher-order networks across all cerebellar and striatal systems.

ACKNOWLEDGEMENTS

Financial support was provided by National Institutes of Health Grants DP50D012109-02 [to A.A., PI (principal investigator)], the National Alliance for Research on Schizophrenia and Depression Young Investigator award (to A.A., PI); and the Yale Center for Clinical Investigation (A.A., PI). Data were provided by the Centers of Biomedical Research Excellence (COBRE) and the Olin Neuropsychiatric Research Center.

REFERENCES

1. Yeo, B.T.*, et al.* The organization of the human cerebral cortex estimated by intrinsic functional connectivity. *J Neurophysiol* **106**, 1125-1165 (2011).
2. Buckner, R.L., Krienen, F.M., Castellanos, A., Diaz, J.C. & Yeo, B.T. The organization of the human cerebellum estimated by intrinsic functional connectivity. *J Neurophysiol* **106**, 2322-2345 (2011).
3. Choi, E.Y., Yeo, B.T. & Buckner, R.L. The organization of the human striatum estimated by intrinsic functional connectivity. *J Neurophysiol* **108**, 2242-2263 (2012).
4. Yang, G.J.*, et al.* Functional hierarchy underlies preferential connectivity disturbances in schizophrenia. *Proc Natl Acad Sci U S A* **113**, E219-228 (2016).
5. Murray, J.D.*, et al.* Linking microcircuit dysfunction to cognitive impairment: effects of disinhibition associated with schizophrenia in a cortical working memory model. *Cereb Cortex* **24**, 859-872 (2014).
6. Stephan, K.E., Baldeweg, T. & Friston, K.J. Synaptic plasticity and dysconnection in schizophrenia. *Biol Psychiatry* **59**, 929-939 (2006).
7. Ray, J.P. & Price, J.L. The organization of projections from the mediodorsal nucleus of the thalamus to orbital and medial prefrontal cortex in macaque monkeys. *Journal of Comparative Neurology* **337**, 1-31 (1993).
8. Haber, S. & McFarland, N.R. The place of the thalamus in frontal cortical-basal ganglia circuits. *Neuroscientist* **7**, 315-324 (2001).
9. Klein, J.C.*, et al.* Topography of connections between human prefrontal cortex and mediodorsal thalamus studied with diffusion tractography. *NeuroImage* **51**, 555-564 (2010).
10. Welsh, R.C., Chen, A.C. & Taylor, S.F. Low-frequency BOLD fluctuations demonstrate altered thalamocortical connectivity in schizophrenia. *Schizophr Bull* **36**, 713-722 (2010).
11. Woodward, N.D., Karbasforoushan, H. & Heckers, S. Thalamocortical dysconnectivity in schizophrenia. *Am J Psychiatry* **169**, 1092-1099 (2012).
12. Anticevic, A.*, et al.* Characterizing thalamo-cortical disturbances in schizophrenia and bipolar illness. *Cereb Cortex* **24**, 3116-3130 (2014).
13. Anticevic, A.*, et al.* Association of Thalamic Dysconnectivity and Conversion to Psychosis in Youth and Young Adults at Elevated Clinical Risk. *JAMA Psychiatry* **72**, 882-891 (2015).
14. Lisman, J.E., Pi, H.J., Zhang, Y. & Otmakhova, N.A. A thalamo-hippocampal-ventral tegmental area loop may produce the positive feedback that underlies the psychotic break in schizophrenia. *Biological Psychiatry* **68**, 17-24 (2010).
15. Holt, D.J.*, et al.* Reduced density of cholinergic interneurons in the ventral striatum in schizophrenia: an in situ hybridization study. *Biol Psychiatry* **58**, 408-416 (2005).
16. Tu, P.C., Hsieh, J.C., Li, C.T., Bai, Y.M. & Su, T.P. Cortico-striatal disconnection within the cingulo-opercular network in schizophrenia revealed by intrinsic functional connectivity analysis: A resting fMRI study. *NeuroImage* (2012).
17. Sarpal, D.K.*, et al.* Baseline Striatal Functional Connectivity as a Predictor of Response to Antipsychotic Drug Treatment. *American Journal of Psychiatry* **173**, 69-77 (2016).
18. Sarpal, D.K.*, et al.* Antipsychotic treatment and functional connectivity of the striatum in first-episode schizophrenia. *JAMA Psychiatry* **72**, 5-13 (2015).
19. Konarski, J.Z., McIntyre, R.S., Grupp, L.A. & Kennedy, S.H. Is the cerebellum relevant in the circuitry of neuropsychiatric disorders? *J Psychiatry Neurosci* **30**, 178-186 (2005).
20. Collin, G.*, et al.* Impaired cerebellar functional connectivity in schizophrenia patients and their healthy siblings. *Front Psychiatry* **2**, 73 (2011).
21. Andreasen, N.C.*, et al.* Schizophrenia and cognitive dysmetria: a positron-emission tomography study of dysfunctional prefrontal-thalamic-cerebellar circuitry. *Proc Natl Acad Sci U S A* **93**, 9985-9990 (1996).
22. Liu, H., Fan, G., Xu, K. & Wang, F. Changes in cerebellar functional connectivity and anatomical connectivity in schizophrenia: a combined resting-state functional MRI and diffusion tensor imaging study. *J Magn Reson Imaging* **34**, 1430-1438 (2011).
23. Rusch, N.*, et al.* Prefrontal-thalamic-cerebellar gray matter networks and executive functioning in schizophrenia. *Schizophr Res* **93**, 79-89 (2007).

24. Wang, L.*, et al.* Disruptive changes of cerebellar functional connectivity with the default mode network in schizophrenia. *Schizophr Res* **160**, 67-72 (2014).
25. Smith, S.M. & Nichols, T.E. Threshold-free cluster enhancement: addressing problems of smoothing, threshold dependence and localisation in cluster inference. *Neuroimage* **44**, 83-98 (2009).
26. Kay, S.R., Fiszbein, A. & Opler, L.A. The positive and negative syndrome scale (PANSS) for schizophrenia. *Schizophrenia Bulletin* **13**, 261-276 (1987).
27. van der Gaag, M.*, et al.* The five-factor model of the Positive and Negative Syndrome Scale II: a ten-fold cross-validation of a revised model. *Schizophr Res* **85**, 280-287 (2006).
28. Baker, J.T.*, et al.* Disruption of cortical association networks in schizophrenia and psychotic bipolar disorder. *JAMA Psychiatry* **72**, 109-118 (2014).
29. Meyer-Lindenberg, A.S.*, et al.* Regionally specific disturbance of dorsolateral prefrontal-hippocampal functional connectivity in schizophrenia. *Arch Gen Psychiatry* **62**, 379-386 (2005).
30. Anticevic, A. & Lisman, J. How Can Global Alteration of Excitation/Inhibition Balance Lead to the Local Dysfunctions That Underlie Schizophrenia? *Biol Psychiatry* (2017).
31. Seeman, P. Atypical antipsychotics: mechanism of action. *Can J Psychiatry* **47**, 27-38 (2002).
32. Seeman, P., Chau-Wong, M., Tedesco, J. & Wong, K. Brain receptors for antipsychotic drugs and dopamine: direct binding assays. *Proc Natl Acad Sci U S A* **72**, 4376-4380 (1975).
33. Seeman, P. & Lee, T. Antipsychotic drugs: direct correlation between clinical potency and presynaptic action on dopamine neurons. *Science* **188**, 1217-1219 (1975).
34. Howes, O.D.*, et al.* Elevated striatal dopamine function linked to prodromal signs of schizophrenia. *Arch Gen Psychiatry* **66**, 13-20 (2009).
35. Mackay, A.V.*, et al.* Increased brain dopamine and dopamine receptors in schizophrenia. *Arch Gen Psychiatry* **39**, 991-997 (1982).
36. Lee, T. & Seeman, P. Elevation of brain neuroleptic/dopamine receptors in schizophrenia. *Am J Psychiatry* **137**, 191-197 (1980).
37. Grace, A.A., Floresco, S.B., Goto, Y. & Lodge, D.J. Regulation of firing of dopaminergic neurons and control of goal-directed behaviors. *Trends Neurosci* **30**, 220-227 (2007).
38. Lodge, D.J. & Grace, A.A. Hippocampal dysregulation of dopamine system function and the pathophysiology of schizophrenia. *Trends Pharmacol Sci* **32**, 507-513 (2011).
39. Gonzalez-Burgos, G. & Lewis, D.A. NMDA Receptor Hypofunction, Parvalbumin-Positive Neurons and Cortical Gamma Oscillations in Schizophrenia. *Schizophrenia Bulletin* **38**, 950-957 (2012).
40. Krystal, J.H.*, et al.* NMDA receptor antagonist effects, cortical glutamatergic function, and schizophrenia: toward a paradigm shift in medication development. *Psychopharmacology* **169**, 215-233 (2003).
41. Barch, D.M. The relationships among cognition, motivation, and emotion in schizophrenia: how much and how little we know. *Schizophrenia Bulletin* **31**, 875-881 (2005).
42. Leitman, D.I.*, et al.* Sensory deficits and distributed hierarchical dysfunction in schizophrenia. *Am J Psychiatry* **167**, 818-827 (2010).
43. Berenbaum, H. & Oltmanns, T.F. Emotional experience and expression in schizophrenia and depression. *Journal of Abnormal Psychology* **101**, 37-44 (1992).
44. Stephan, K.E., Friston, K.J. & Frith, C.D. Dysconnection in schizophrenia: from abnormal synaptic plasticity to failures of self-monitoring. *Schizophrenia bulletin* **35**, 509-527 (2009).
45. Calderone, D.J.*, et al.* Comparison of psychophysical, electrophysiological, and fMRI assessment of visual contrast responses in patients with schizophrenia. *Neuroimage* **67**, 153-162 (2013).
46. Horga, G.*, et al.* Dopamine-Related Disruption of Functional Topography of Striatal Connections in Unmedicated Patients With Schizophrenia. *JAMA Psychiatry* **73**, 862-870 (2016).
47. Fornito, A.*, et al.* Functional Dysconnectivity of Corticostriatal Circuitry as a Risk Phenotype for Psychosis. *JAMA psychiatry (Chicago, Ill.)* (2013).
48. Shinn, A.K., Baker, J.T., Lewandowski, K.E., Ongur, D. & Cohen, B.M. Aberrant cerebellar connectivity in motor and association networks in schizophrenia. *Front Hum Neurosci* **9**, 134 (2015).
49. Di Martino, A.*, et al.* Aberrant striatal functional connectivity in children with autism. *Biol Psychiatry* **69**, 847-856 (2011).

50. Harrison, B.J.*, et al.* Altered corticostriatal functional connectivity in obsessive-compulsive disorder. *Archives of General Psychiatry* **66**, 1189-1200 (2009).
51. Dandash, O.*, et al.* Altered striatal functional connectivity in subjects with an at-risk mental state for psychosis. *Schizophr Bull* **40**, 904-913 (2014).
52. Cubillo, A.*, et al.* Reduced activation and inter-regional functional connectivity of fronto-striatal networks in adults with childhood Attention-Deficit Hyperactivity Disorder (ADHD) and persisting symptoms during tasks of motor inhibition and cognitive switching. *J Psychiatr Res* **44**, 629-639 (2010).
53. Anand, A., Li, Y., Wang, Y., Lowe, M.J. & Dzemidzic, M. Resting state corticolimbic connectivity abnormalities in unmedicated bipolar disorder and unipolar depression. *Psychiatry Res* **171**, 189-198 (2009).
54. Anticevic, A.*, et al.* Global resting-state functional magnetic resonance imaging analysis identifies frontal cortex, striatal, and cerebellar dysconnectivity in obsessive-compulsive disorder. *Biol Psychiatry* **75**, 595-605 (2014).
55. Parent, A. & Hazrati, L.N. Functional anatomy of the basal ganglia. I. The cortico-basal ganglia-thalamo-cortical loop. *Brain Res Brain Res Rev* **20**, 91-127 (1995).
56. Alexander, G.E., DeLong, M.R. & Strick, P.L. Parallel organization of functionally segregated circuits linking basal ganglia and cortex. *Annual Review of Neuroscience* **9**, 357-381 (1986).
57. Middleton, F.A. & Strick, P.L. Cerebellar projections to the prefrontal cortex of the primate. *J Neurosci* **21**, 700-712 (2001).
58. Schmahmann, J.D. & Caplan, D. Cognition, emotion and the cerebellum. *Brain* **129**, 290-292 (2006).
59. Stoodley, C.J. The cerebellum and cognition: evidence from functional imaging studies. *Cerebellum* **11**, 352-365 (2012).
60. Decety, J., Sjoholm, H., Ryding, E., Stenberg, G. & Ingvar, D.H. The cerebellum participates in mental activity: tomographic measurements of regional cerebral blood flow. *Brain Res* **535**, 313-317 (1990).
61. Andreasen, N.C. & Pierson, R. The role of the cerebellum in schizophrenia. *Biol Psychiatry* **64**, 81-88 (2008).
62. Sokolov, A.A., Miall, R.C. & Ivry, R.B. The Cerebellum: Adaptive Prediction for Movement and Cognition. *Trends Cogn Sci* **21**, 313-332 (2017).
63. Barch, D.M.*, et al.* Selective deficits in prefrontal cortex function in medication-naive patients with schizophrenia. *Arch Gen Psychiatry* **58**, 280-288 (2001).
64. Camchong, J., Macdonald, A.W., Bell, C., Mueller, B.A. & Lim, K.O. Altered functional and anatomical connectivity in schizophrenia. *Schizophrenia bulletin* **37**, 640-650 (2011).
65. Scholtens, L.H., Schmidt, R., de Reus, M.A. & van den Heuvel, M.P. Linking macroscale graph analytical organization to microscale neuroarchitectonics in the macaque connectome. *J Neurosci* **34**, 12192-12205 (2014).
66. Murray, J.D.*, et al.* A hierarchy of intrinsic timescales across primate cortex. *Nat Neurosci* **17**, 1661-1663 (2014).
67. Schnack, H.G.*, et al.* Can structural MRI aid in clinical classification? A machine learning study in two independent samples of patients with schizophrenia, bipolar disorder and healthy subjects. *Neuroimage* **84**, 299-306 (2014).
68. Davatzikos, C.*, et al.* Whole-brain morphometric study of schizophrenia revealing a spatially complex set of focal abnormalities. *Arch Gen Psychiatry* **62**, 1218-1227 (2005).
69. Kawasaki, Y.*, et al.* Multivariate voxel-based morphometry successfully differentiates schizophrenia patients from healthy controls. *Neuroimage* **34**, 235-242 (2007).
70. Ardekani, B.A.*, et al.* Diffusion tensor imaging reliably differentiates patients with schizophrenia from healthy volunteers. *Hum Brain Mapp* **32**, 1-9 (2011).
71. Iwabuchi, S.J., Liddle, P.F. & Palaniyappan, L. Clinical utility of machine-learning approaches in schizophrenia: improving diagnostic confidence for translational neuroimaging. *Frontiers in psychiatry* **4**, 95 (2013).
72. Insel, T.*, et al.* Research domain criteria (RDoC): toward a new classification framework for research on mental disorders. *Am J Psychiatry* **167**, 748-751 (2010).